

*On the Use of a New York City  
Water Tank as a Cosmic Ray Detector*

Brandon Hsieh

Guang-Yu Zhu

Neil Zimmerman

EE 163 Senior Thesis

Department of Electrical Engineering

The Cooper Union for the Advancement of Science and Art

May, 2004

## *Abstract*

The source of ultra high energy cosmic rays is one of the foremost mysteries in the field of astrophysics. Due to their size, wide spatial distribution, and density, NYC rooftop water tanks present an unparalleled infrastructure for a cosmic ray air shower detector array that would have formidable scientific relevance. We have designed an economic implementation of a water Cherenkov radiation detection system that is ready to be tested in the water tank on the roof of the Cooper Union Engineering Building. To reach this point, considerations of photomultiplier response, materials, and construction were addressed.

## *Chapter 1: Introduction*

### **1.1 Ultra High Energy Cosmic Rays**

Cosmic rays are subatomic particles traveling through space at relativistic speeds. The mechanism of their acceleration is what most intrigues physicists and astronomers. By locating the source of these particles as they arrive from distant energetic events, we can gain a greater understanding of the fundamental processes that govern the most extreme objects in the universe. Ultra high energy (UHE) cosmic rays are set aside in a unique category as particles – protons and heavier nuclei – whose individual energy is greater than  $10^{19}$  eV. No theory has conclusively explained how such high momentum is obtained without conflicting with widely accepted features in our current model of the cosmos.

Our understanding of UHE cosmic rays is limited by the scarcity of recorded encounters—this is due to the fact that UHE cosmic ray events are so infrequent and the fact that the instrumentation of the field is still immature [1]. As mentioned above, there are formidable theoretical difficulties that astrophysicists face in explaining the existence of UHE cosmic rays. Astronomers have not been able to identify the location of the cosmic ray sources, since of the limited encounters that have been recorded, none of the instrumentation had the necessary precision. In addition, it is indeterminate whether or not UHE cosmic rays shower the Earth from all directions. In other words, UHE cosmic rays might be isotropic. The possibility that the arrival directions do not reflect the distribution of matter of our galaxy, the Milky Way, would imply that UHE cosmic rays are from far more distant sources. However, a popular theory states that cosmic rays should originate within 30 million light years, because across any greater distance the cosmic microwave background radiation would interact with the UHE cosmic rays to such a degree as to place an even more extraordinary lower bound on their initial energy. Many astronomers hesitate to increase this lower bound because it multiplies the difficulty in explaining processes that produce particles with several orders of magnitude more energy than can be explained by any known mechanism. The theory of cosmic rays interacting with the microwave background radiation is the Greisen-Zatsepin-Kuz'min (GZK) cutoff, which predicts that cosmic rays with an energy of  $5 \times 10^{19}$  eV should be severely attenuated, having a mean free path of about 100 million light years. Therefore, a source of UHE cosmic rays would probably

be within the galactic neighborhood. By neighborhood, we mean the Virgo Supercluster, which is the 200 million light year diameter region containing the Milky Way, among several thousand other galaxies. One example of a theory that proposes sources within range to prevent conflict with the GZK cutoff is acceleration caused by Active Galactic Nuclei (AGNs). For example, some astronomers believe that the AGN radio source Cen-A could accelerate protons to an energy of  $10^{21}$  eV [2].

Theorists have also attempted to explain how particles can accelerate to such high energies within the Milky Way. In 1949, Enrico Fermi devised a mechanism by which a free nucleus might be accelerated to great velocities. He stated “protons speed up by bouncing off moving magnetic clouds in space” [3]. However, taking the size of our galaxy into account, and its available magnetic field strength, the Fermi mechanism cannot produce particles with energies above  $10^{15}$  eV. Therefore, it is apparent that the kind accelerator needed to produce UHE cosmic rays does not exist within the Milky Way [4].

Despite the GZK cutoff, we cannot eliminate the possibility that sources beyond the galactic neighborhood are capable of accelerating particles to the requisite energy. Of the more distant objects that are candidates for producing UHE cosmic rays, quasars are most often considered. In 1998, NYU physicist Glennys Farrar published an article entitled “Correlation Between Compact Radio Quasars and Ultrahigh Energy Cosmic Rays” in the *Physical Review Letters*. Glennys Farrar proposed that the origins of UHE cosmic rays are distant quasars. Farrar and Peter Bierman of the Max Planck Institute for Radio Astronomy in Bonn found that the projected direction of origin of the five most energetic cosmic rays ever detected on Earth roughly corresponded with the location of five radio-loud quasars [5].

Gamma Ray Bursts (GRBs) are another major possible source for the production of UHE cosmic rays. A mystery in their own right, GRBs emit gamma radiation that can be detected by satellite instruments, arriving about once a day from random directions and lasting from 4 milliseconds to 1000 seconds. Although the causes and the location of GRBs are unknown, it is believed that these phenomena might be the same events accelerating particles to energies on the order of  $10^{20}$  eV. If GRB sources are distributed within the local galactic neighborhood, the GZK cutoff would be satisfied. As more UHE cosmic ray events are collected in the future, a

correlation between the sky locations of GRBs and UHE cosmic rays would be extremely compelling [6].

There is a dire need for more experimental data of UHE cosmic ray events, primarily in order to determine the direction of origin of the particles. Even with poor angular resolution, determining if there are any large-scale anisotropies in the arrival of cosmic rays with respect to the Milky Way galaxy would be crucial in determining the scale of distance on which theorists should focus.

## **1.2 Extensive Air Showers**

Although there is little evidence telling where UHE cosmic rays begin, we do have a fair understanding of how their journey ends. Upon impact with atmospheric nuclei, cosmic rays disperse their energy towards the surface of the Earth in a phenomenon known as an extensive air shower (EAS). Empirical data have shown that EAS events occur when the primary cosmic ray has an energy above  $10^{14}$  eV [7]. The most significant propagators of this energy reaching the surface are gamma rays, electrons, and muons. Because the trajectory of these particles at the core of the shower is aligned with that of the incident particle, the direction of origin can be inferred if data from spatially separated detectors are correlated. It should be noted, however, that even when the trajectory of a cosmic ray in the upper atmosphere has been determined, we cannot simply extend an imaginary line in space to identify its source. Because the cosmic ray is essentially a charged particle, it is subject to magnetic interactions with Earth, galactic magnetic fields, and possibly intergalactic magnetic fields. Fortunately, there is evidence that these fields are not strong enough to deflect the highest energy cosmic rays significantly [8]. Still, astrophysicists must take galactic magnetic fields into account when tracing back the source. In addition to the trajectory, the energy and composition of the incident particle can also be determined from the data collected by detector instruments.

When the primary cosmic ray collides with a nucleus in the upper atmosphere (about 20 km above the earth's surface), high-energy pions and gamma photons are produced (see Figure 1.1). Pions are non-elementary particles that normally act as nuclear force carriers between neutrons and protons [9]. Pions have a lifetime of a few tens of nanoseconds, and either rapidly decay into muons or collide with another nucleus. Muons are the most energetic component of the air

shower that we can detect at the Earth's surface. The term muon refers to a particle having the same magnitude of charge as an electron, but about 200 times the mass. The highest energy muons in an extensive air shower correspond to the decay of the highest energy pions, and therefore give us information about the early development of the EAS. Just as the counterpart of the electron is the positron, the counterpart of the muon (negatively charged) is the antimuon (positively charged). The muon is unstable and decays into an electron, a muon-type neutrino and an electron-type neutrino. Similarly the antimuon decays into a positron, a muon-type antineutrino and an electron-type antineutrino. Muons have a much longer lifetime than pions, lasting 2.2 microseconds. The average energy of a muon created in an EAS event is 4 GeV. As muons travel at relativistic speeds with high energy, time dilation permits the particles to hit the Earth's surface before they decay. EAS muons cause little interaction when they penetrate materials, partly because they are too heavy to be greatly deflected by atomic electrical fields.

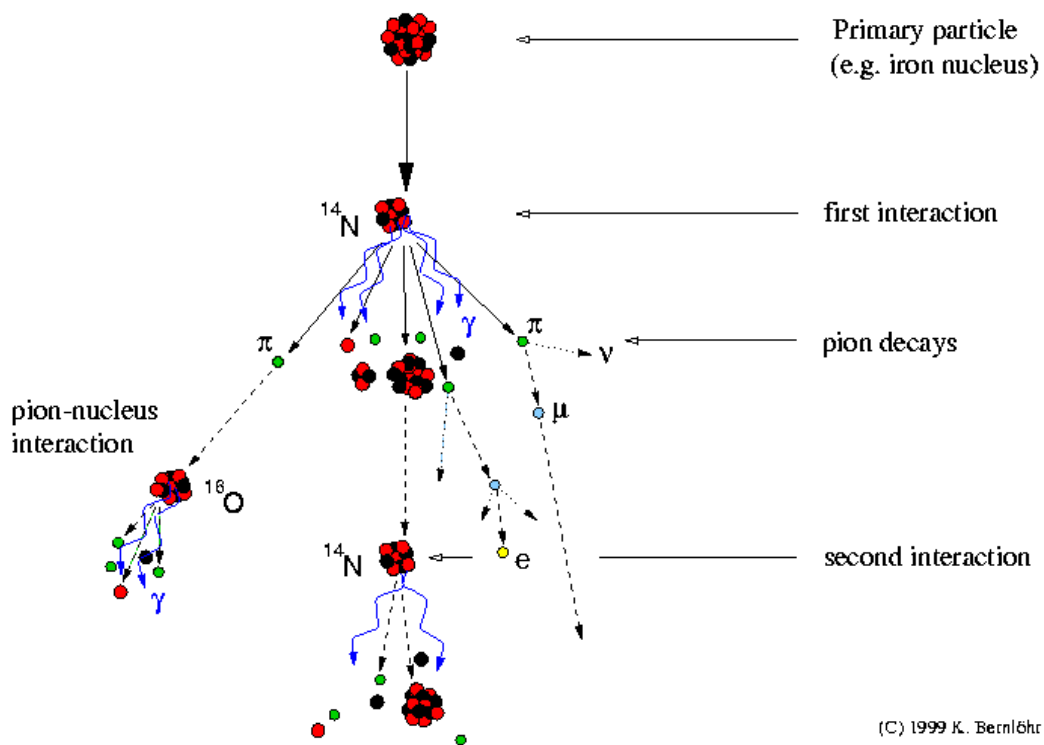


**Figure 1.1** Development of cosmic ray air showers [10].

Since we only measure the secondary particles on the surface, we need to know the relationship between the secondary particles and the cosmic ray in order to extract useful information. To accomplish this, various research institutions have created Monte Carlo computer simulations based on first principles to model the formation and propagation of EAS events. The temporal and spatial distribution of each type of particle arriving at the ground (muons, electrons, and gamma rays) is shown by these simulations to have strong relationships with the energy and composition of the original cosmic ray [11].

### 1.3 Extensive Air Shower Detection with a Water Cherenkov Detector

The most efficient method of detecting EAS particles is the water Cherenkov detector. This technique relies on the Cherenkov radiation effect, which is the light that is produced when a charged particle passes through water at a speed greater than the speed of light specific to water. The traveling particle polarizes the molecules, causing them to rotate and then restore their orientations, resulting in the emission of electromagnetic wavelets. If the charged particle is moving faster than  $\sim 0.75c$ , the speed of light in water, then constructive interference will occur at angle of  $\arccos(0.75/\beta)$  from the reverse trajectory of the particle, where  $\beta$  is the ratio of the speed of the particle to  $c$  (see Figure 2). Therefore, the light of peak intensity is radiated in wavefronts in the shape of an open cone with the pointed end forward [12]. For a typical crossing muon, with an energy on the order of 1 GeV, the speed of the particle approaches that of light, and therefore will cause a Cherenkov emission angle of  $41^\circ$ .

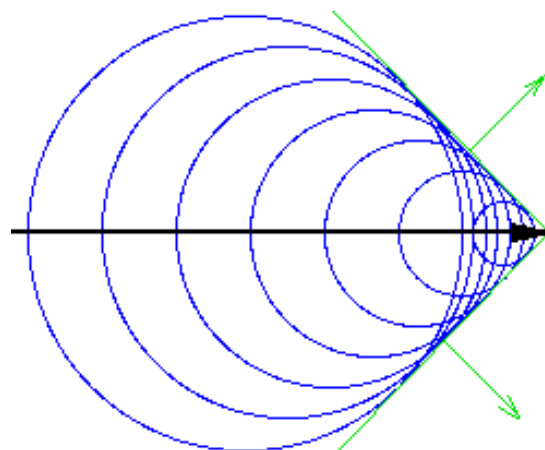


**Figure 1.2** The creation of Cherenkov radiation [13].

The quantity of Cherenkov radiation produced is proportional to the path length through the container of the medium. This is seen more precisely in equation 1.1, the formula for the yield of Cherenkov photons.

$$\frac{dN}{dx} = 2\pi\alpha \left(1 - \frac{1}{\beta^2 n^2}\right) \times \int \frac{1}{\lambda^2} d\lambda \quad \dots(1.1)$$

Here  $N$  represents the number of photons,  $x$  the path length of the relativistic particle,  $\beta$  the ratio of the speed of the particle to  $c$ ,  $\lambda$  the wavelength of light,  $n$  the refractive index of the medium, and  $\alpha$  the fine structure constant [14]. As shown by this formula, the emission of Cherenkov radiation is inversely dependent on wavelength. However, taking into account the absorption properties of water, it becomes apparent that only a small range of wavelengths will yield significant amounts of Cherenkov radiation in a water container. The absorptive strength of water is measured in a quantity called absorption length, which is the mean free path that a particle can travel without an inelastic collision occurring. For pure water, this value reaches its peak between 300 and 500 nm. As wavelength decreases from 300 nm to beyond the ultraviolet range, the mean free path of light in water approaches zero. Therefore the light sensor in a water Cherenkov detector should have optimal sensitivity in between 300 nm and 500 nm. However, in practice the presence of dissolved solids in the water can dramatically reduce the transmission of light from the ultraviolet region up to around 360 nm. In such cases the range of available Cherenkov light would be reduced to the violet-blue region of the spectrum.

Although they have other uses in the fields of nuclear and particle physics, many Cherenkov detectors have been built solely for the purpose of detecting EAS particles. However, one counter by itself, although capable of detecting an essentially continuous stream of particles arriving as a result of moderate EAS events, is not capable of quantifying either the energy or the atmospheric trajectory of a cosmic ray. One might suppose that the intensity of the light recorded by the water Cherenkov detector would have a close relationship with the energy of the original cosmic ray. However, because the energy of the primary cosmic ray energy becomes diffused in the air shower over a width of several kilometers, reconstructing the event requires information to be collected over a much larger area than a single instrument [15]. The air shower can be thought of as a wavefront, similar to an electromagnetic plane wave in that the time of ground arrival varies with location, dependent on the angle of incidence. If many water

Cherenkov detectors can document the precise time of arrival of particles, then analysis of their combined data may enable the identification, above the "noise" of random particle counts, of the fingerprint of an EAS wavefront, and therefore the direction of the cosmic ray when it entered the atmosphere. The energy of the cosmic ray can be determined from the distribution of arriving particles measured by the water Cherenkov detectors – the lateral profile of the air shower core has a strong relationship to the energy of the cosmic ray [16]. This is because the total amount of each species of particle created in an EAS is strongly related to the primary energy. Although counting the total amount of EAS particles is not feasible, looking at the density of particle interactions recorded at ground level as a function of distance from the shower core allows the primary energy to be estimated [17]. By comparing the lateral distribution of showers with computer simulations, the height of the EAS maximum can also be determined. This height is related to the composition of the primary cosmic ray – for example, it would indicate the difference between a Helium nucleus and an Iron nucleus for the primary particle. The composition of the primary particle is also an important parameter in determining the source of the radiation.

For statistical considerations, it is best to have a large collecting area of water to maximize the amount of air shower particles incident on the container. And, because the showers can arrive from large zenith angles, their vertical dimension should be comparable to their lateral size. Therefore, a water container of large volume will be of greatest use in studying air showers. Aside from the properties of the individual water Cherenkov detectors, two main factors affect the performance of a detector array: the spacing between detectors and the overall area. Because the wavefront of an EAS is sharper and more uniform at the center, it is beneficial to have smaller detector spacing in order to have greater time resolution wherever the core of the shower lands. This would permit the direction of origin to be determined with higher precision [18]. At the same time, larger overall array area allows the measurement of more events, especially the higher energy ones which are much more rare (the central axes of  $10^{20}$  eV showers have an average arrival rate of  $1/\text{km}^2$  per century) [19].

## **1.4 New York City's Rooftop Water Tanks**

New York City has one of the older water systems in the United States. While cities that boomed during a later time period had the advantage of slightly more modern techniques, New York City relies on gravity to transport water from reservoirs in upstate New York through pipes that are of a wider than optimal gauge [20]. The resulting pressure is 45 to 60 pounds per square inch, which in the city is only enough to reach six stories on average [21].

Since the 19th century, one solution has remained the most cost-effective and simple, and that is the wooden rooftop water tank. Gathering water from ground pumps, the tank acts as an intermediate stage between the public supply and the tall building, supplying all of the needed water with the force of gravity alone. The cylindrical wall of a typical tank is made of vertical wooden staves (either redwood or cedar), 2.5" thick, held together by a series of galvanized iron hoops encircling the outside [22]. There is no adhesive required, because when the tank is filled with water, the wood expands to close any gaps. The tanks have an expected lifetime of 25-30 years, but have been known to last quite a bit longer [23]. In all of NYC, there are approximately 10,000 wooden water tanks in operation. Every year, about 100 are either built or replaced [24].

Although a typical wooden water tank holds 10,000 gallons of water, their volumes range from 3,500 gallons to 50,000 gallons, depending on the size of the building and the purpose of the tank. According to Fire Code of the City of New York, every residential building over six stories high that doesn't have access to two water mains must have 3,500 gallons of water ready for firefighters to access in case of emergency [25]. Generally, the only buildings that have access to two water mains are those that cover the corner of a block. As a result of this law, many buildings use rooftop water tanks as a solution to this requirement [26]. Although some buildings use two or more tanks for different purposes, one tank is often used to supply both potable water and emergency supply. This is accomplished by using multiple output pipes at different levels in the tank.

## **1.5 The Dawning of a Cosmic Ray Experiment in New York City**

Glennys Farrar, Director of the Center for Cosmology and Particle Physics at NYU, is a theorist who studies cosmic rays, in addition to other topics in astrophysics and particle physics.

She is also the project leader of the New York Schools Cosmic Particle Telescope, which is an organization started in 2002 to distribute small EAS particle detectors to high schools around the city. This enables science education beyond the standard curriculum, and the foundation of an array of fairly large area to permit observations of air showers. Although only a small number of detectors have been deployed thus far, Glennys Farrar has another idea in the meantime. When she looks at the rooftops of the New York skyline, she sees scores of wooden water tanks waiting to be turned into water Cherenkov detectors, forming an unusual but powerful EAS detection array.

The requisites for a premiere EAS detection array using NYC's water tanks are more or less in place. The overall area that the water tanks span is large enough to compete with any EAS array in existence because NYC has an area of  $831 \text{ km}^2$  [27]. This is comparable to what is by far the largest EAS detector array, the Pierre Auger Observatory in Argentina, which will have an area of  $3000 \text{ km}^2$  when completed [28]. Empirical data have shown the frequency of  $10^{20} \text{ eV}$  air showers to be one per  $\text{km}^2$  per century, and therefore one can estimate the rate of  $10^{20} \text{ eV}$  showers impinging on NYC:

$$\text{frequency} \times \text{area} \approx 1 \text{ event}/(1 \text{ km}^2 \times 10^2 \text{ years}) \times 10^3 \text{ km}^2 \approx 10 \text{ events/year.}$$

However, that estimation assumes that the area of NYC is compacted into one chunk. But in fact, as one can verify from a map, the area spanned by the five boroughs of NYC is quite a bit greater when the irregularities of the landmasses and surface occupied by bodies of water are also taken into account. An analysis of how much effective area this would provide for the purposes of EAS detection would be useful in upgrading the evaluation of the performance of the array. This is not a trivial computational matter because the lateral spread of the EAS needs to be taken into account. If detectors on separate landmasses are separated by large distances, they can no longer share the detection of the same EAS event. Normally the radius of the air shower arriving at the surface is confined to about 5 km.

The water tanks for the Pierre Auger Observatory are custom built. Obviously, the number of tanks placed in such an array is a critical constraint on the project's budget, and in those circumstances a compromise must be found between array resolution and cost. The final Pierre Auger Observatory design has tanks separated by approximately 1.5 km on a triangular grid [29]. Although we are still in the process of trying to obtain a map of the exact locations of

NYC's water tanks, the very rough order of magnitude approximation of 10,000 wooden water tanks fitted into a square grid of area  $1000 \text{ km}^2$  would yield a mean separation of  $\sqrt{(1000 \text{ km}^2)/\sqrt{(10,000)}} \approx 0.3 \text{ km/tank}$ . We cannot assume that every building with a water tank would participate in the experiment. But, there are certain considerations that might compensate for an unremarkable average separation between tanks. Firstly, the density of water tanks in certain parts of the city, especially Manhattan, can still provide a region of unprecedented resolution, with current water tank spacing that can be conservatively estimated to be on the order of 100 m. The island of Manhattan, which has an area of  $57 \text{ km}^2$ , is subject to one  $10^{20} \text{ eV}$  EAS event every two years and over 50 EAS events per year resulting from  $10^{19} \text{ eV}$  primaries [30]. Manhattan's potential detector density is scientifically valuable because it would theoretically provide significant information about the air shower trajectory. Secondly, the smaller detectors of the kind originally proposed by the NYSCPT can still be used in conjunction with the water tanks, so that buildings that do not have water tanks can still contribute to the collection of air shower data. The vast majority of NYC high school and middle school buildings are not above the six floors that would require the use of a water tank, and therefore their participation, being a primary goal of the NYSCPT, could be realized with the use of smaller detectors on the school rooftops. The added data from the smaller detectors could be correlated with that of the Cherenkov detectors, adding a significant boost to the overall resolution.

The Pierre Auger Observatory water tanks were designed with the aid of computer simulation and information from the older Haverah Park experiment. Therefore, a comparison of the Auger tank dimensions with those of the NYC wooden tanks can be used as a basis of assessing the scientific suitability of the latter. The Auger designers' computer simulations indicated that with a detector spacing of 1.5 km, a tank with a horizontal area of  $10 \text{ m}^2$  is sufficient for the study of the highest energy cosmic rays [31]. A typical NYC water tank, having a base area of  $12.6 \text{ m}^2$ , matches the Auger tank collecting area.

In order to demonstrate the scientific relevance of using NYC water tanks as an array of cosmic ray detectors, it is necessary to find a method by which events can be time stamped with precision equal to or better than existing instruments. The most precise array of this kind is the Auger Observatory, which uses a GPS receiver on each tank to attain a root mean square precision of 10 ns.

At the time that the Pierre Auger Observatory was still being designed, M. A. DuVernois of Pennsylvania State University proposed that each detector use both GPS and Glonass (the Russian equivalent of GPS) in parallel to boost the time stamp precision [32]. In this system, a reference station in view of GPS and Glonass keeps the maser time of the experiment. The reference station radios a time correction to each detector with known relative position, which also receives both GPS and Glonass. Such a system would have offered a root mean square precision of 2 ns. Although the Glonass has since fallen out of operation, the European satellite constellation Galileo, scheduled to be launched by the end of the decade, promises even more precision for combination receivers [33]. We propose implementing this method in the future NYC cosmic ray detector array. According to DuVernois' proposal, the total cost of a time-transfer system is reasonable. For example, a GNSS-300 master station with software costs approximately \$30,000. The cost of a combination receiver would be about \$200 for each detector.

## **1.6 Our Water Cherenkov Detector**

It is to the advantage of this project that the wooden water tanks used on the roofs of New York City are for the most part of identical form, except for variations in size. This increases the feasibility of a mass producible kit and procedure that could be generalized for all interested parties. Glennys Farrar believes that if the procedure to adapt each tank as a water Cherenkov detector can be proven to be completed for around \$5,000, there is a good chance of obtaining funding to expand the experiment to as many water tanks as possible.

The objective for our project within this academic year was the demonstration of the operation of one NYC water tank as a Cherenkov detector in such a way that can be inexpensively replicated for many water tanks. Although not scientifically interesting, the results of our work will be important in the grant proposal by the New York Schools Cosmic Particle Telescope to create many NYC water tank detectors in the future. The basic form of our detector is similar to that implemented in the Pierre Auger Observatory water Cherenkov detectors. Like the Auger Observatory, our design calls for 2-3 photomultiplier tubes (PMTs) to be submerged in the water tank, acting as Cherenkov radiation sensors. The Auger detectors have a reflective liner on the interior surface of the tank, made of Tyvek film, so that Cherenkov radiation is

approximately evenly distributed to the sensors throughout the tank [34]. Unfortunately, because we were unable to gain access to an emptied water tank, we have not yet tested a reflecting lining. However, panels of MYLAR film sandwiched in polyethylene or propylene resting along the walls of the tank would be a safe (inert) and affordable solution to this problem. Burle Industries provided us with a generous discount on one of their PMT models, the 83049-542, which has a relatively large 3 inch diameter photocathode. Therefore, we have designed and constructed our prototype around this device, and experimentally characterized its response to Cherenkov radiation. The significance of having a sensor with large aperture is that we can sample the Cherenkov radiation over as wide an area as possible inside the tank. Ideally, the water container would be surrounded by light sensors, as is done in the Super-Kamiokande neutrino experiment [35]. However, the idea of using more than 3 PMTs should not be eliminated, and may be seriously considered once the Cherenkov light response of a NYC water tank with reflective lining has been measured. The use of more, or even larger PMTs might compensate for shortcomings of NYC tanks such as water clarity.

Thanks to successful discussions with the Isseks tank company and the NYU Facilities Manager, we will soon be able to install our prototype detector inside a wooden standpipe supply tank on the roof of an NYU building. Because of the fact that most of the wooden water tanks in NYC are used for domestic supply, all of the materials we have chosen in our design are officially approved for contact with drinking water. Thanks to the help of Michelle Norris, a Cooper Union alumna, we are in the process obtaining the specific legal approval needed from the New York City Department of Buildings in order to streamline the installation of multiple detectors throughout the city.

## *Chapter 2: Trash Can Cherenkov Detector*

To create a laboratory scale water Cherenkov detector, we chose a galvanized steel trash can. Many practical challenges were resolved in order to create this vital testing environment for our electronics. Although plastic trash cans are readily available, the design criteria for a detector are more easily satisfied using a metal tank. The detection of Cherenkov radiation must be completed in an optically isolated container, and even opaque plastics permit some optical transmission. Metal, on the other hand, lacks translucence and steel, in particular, has a reflectivity on the order of 90%. This reflectivity serves to maximize the amount of Cherenkov radiation incident on the photomultiplier tube (PMT) in the tank. We chose a galvanized steel trash can with a height of 30 inches and a top diameter of 20.5 inches (Figure 2.1).



**Figure 2.1** Trash Can.

Although galvanized steel is opaque, the join between the trash can handle and lid appeared to be a potential source of light leaks. We were able to seal this area with the use of an epoxy. In addition to sealing the light leaks, it was necessary to make the can watertight. We attempted several methods to seal the water leaks in the can, but none were successful. After our first inspection, we expected the seams where the two halves of the can joined to be a primary source for water leaks. We lined these two seams and the edge where the body met the floor of the tank with RTV silicone caulk. After allowing 24 hours for the caulk to dry, we tested the seals by slowly filling up the can with water. We found water dripping at the intersection

between the vertical seam and the floor of the can. We removed the caulk and repeated the procedure using RTV silicone #2, which should create a stronger bond with galvanized steel. However, leaks remained, and other procedures for creating a water tight tank were considered.

We applied aluminum patches using epoxy to the intersection of the wall and floor seams on the exterior surface of the can, but this application failed to eradicate the problem. We also tried plumber's glue as a final resort. Welding remained as one method to seal the can, but we determined that it would be preferable to identify a simple and quick solution. We chose to use a transparent polyethylene sheet that easily eliminates the water leak problem while preserving the reflectivity of the can interior (see Figure 2.2).

We made more modifications to the tank in order to install the PMT in the tank and create a light seal between the lid and can which also permitted easy access to the interior. We first attempted to optically seal the area where the lid made contact with the top edge of the trash can by gluing rubber tubing to the outside of the can. However, the silicone caulk did not act as an effective adhesive, and repeated use of the lid caused most of the tubing to peel off. We achieved much better results by folding thin foam sheets over the rim of the can and securing them in place with duct tape. The foam sheets provided a snug fit for the lid that remained resilient throughout all further experiments, and proved to provide a light-tight seal.

We designed the placement of the PMT to permit access to its base for easy modifications to any connection. In addition, we did not want to use adhesives on the surface of the PMT, since this would complicate the reuse of the device in future experiments. We reached these requirements by supporting the PMT so that it faced inwards from a hole in the side of the can, fixed in place only by the pressure of compressed foam sheets. We cut a 2.5" diameter circular hole in the middle of the wall of the can, large enough for the collar of the PMT to fit through. The socket for the PMT consisted of two pieces. First there was a 2" long, 4" diameter aluminum tube, designed to hug the sides of the back of the PMT. Secondly there was the square faceplate, with a hole cut for the PMT to be inserted through. We fastened the faceplate to the surface of the can around the hole with six small bolts and nuts. The faceplate provided a flat surface on which we cemented the aluminum tube so that it was perpendicular to the can (see Figure 2.3). We sealed the gaps in between the exterior surface of the trash can and the faceplate with epoxy and caulk, thus ensuring optical insulation.



**Figure 2.2** Polyethylene barrier.

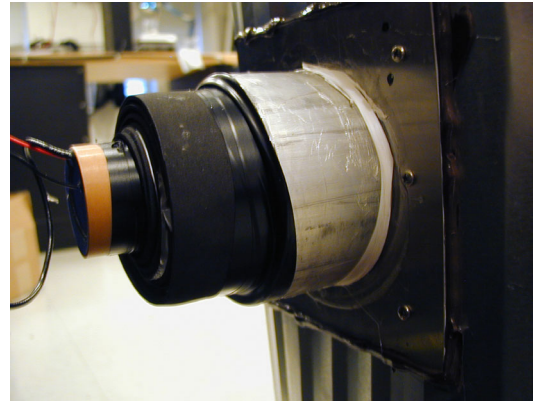


**Figure 2.3** PMT socket.

We were next presented with the challenge of sealing the gap in between the PMT and the aluminum in order to maintain optical insulation. We covered the outside of the PMT with masking tape, and then wrapped the PMT with elastic foam sheets (also shown in Figure 2.3). These sheets were identical to the ones used around the top edge of the trash can. We then glued the inside edges of the foam wrapping to the surface of the trash can with water resistant epoxy.

The trash can detector was tested inside a darkened room with an external supply voltage of 3.0 Volts applied to the PMT. Note that the PMT has an internal voltage multiplier to supply the high voltage necessary for the device to operate. This supply voltage, which yields an internal supply of 400 V, was chosen after consulting the manufacturer of the PMT to ensure that even with substantial light leaks the device would not be damaged. We observed the anode of the PMT on the oscilloscope while switching a flashlight on and off at different points around the can. We found that the response fluctuated randomly by several hundred millivolts when the flashlight was pointed around the lid of the trash can. The cause of this was attributed to the fact that the polyethylene sheet, which extended from the inside of the can to the outside, would guide light along the sheet no matter how much tension existed between the lid and the can. We trimmed the plastic up to the bottom edge of the lid and sealed the plastic from outside light with duct tape. Repeating the procedure of monitoring the anode while moving the flashlight, we found that the response of the PMT remained flat. By connecting the PMT anode to the 1 M $\Omega$  jack of an oscilloscope, we were able to capture a continuous stream of pulses with negative peaks. The peaks varied between just below the noise level (around -10 mV for this

oscilloscope) and -2 V. We improved this setup by connecting the anode to an oscilloscope with a  $50\ \Omega$  input jack to match the impedance of the anode cable.

To verify that our detector was observing air shower particles, we created a separate detector using an organic scintillation paddle, and tested the two for coincidence (see Figure 2.4). The procedure of setting up a basic scintillation detector was followed from a document written by Dietrech Z. Washington of Columbia University's Nevis Laboratory [36]. Our detector used a 2 feet x 8 inch x 0.5 inch block of translucent organic scintillator to produce light upon the arrival EAS muons. First, we wrapped the scintillator paddle in a layer of aluminum foil. Over the center of the broad side of the paddle, a hole slightly smaller than the diameter of the photocathode of our PMT was cut into the aluminum foil using a razor blade. Next we wrapped the entire paddle in electrical tape, except for the hole. Before placing the PMT face down over the hole in the foil, a dab of optical grease was applied to the photocathode, thereby matching the index of refraction between the glass and the scintillator. Next the joint between the PMT and the paddle was sealed with electrical tape, creating a reasonably light-tight enclosure of the paddle and the bulb of the PMT.

To record data with the trash can setup and future water Cherenkov experiments, we borrowed a Quarknet DAQ card from the Columbia University Physics Department. The card was designed at Fermilab for economic implementation of cosmic ray detectors in schools, and it has four channels of time-to-digital converters with a precision of 1 nanosecond. The threshold of each channel is independently adjustable with a potentiometer, between 0 and  $-75\ \text{mV}$ . Through an RS-232 serial port interface, we adjusted the time window of coincidence to the device's minimum, 48 nanoseconds. After we placed the scintillation detector on top of the lid of the trash can, we observed the accumulation of coincidence counts on the Quarknet display.



**Figure 2.4** Coincidence setup.

In addition, we were later able to observe coincidences directly on an oscilloscope. As a result, we were confident that our trash can Cherenkov detector was indeed detecting EAS particles.

## *Chapter 3: Detection and Photomultiplier Measurements*

### **3.1 Light Detecting Device**

To choose the light sensor for our water tank Cherenkov detector, we considered two categories of devices that had the required sensitivity – the avalanche photodiode and the vacuum photomultiplier tube. In both cases we are concerned with the same operating principle – the amplification of charge emitted due to the photoelectric effect. In a photomultiplier, photoelectrons emitted from the cathode are multiplied by secondary electron emission from a series of dynodes at successively higher potentials. In an avalanche photodiode, electron-hole pairs are created by incident light in a PN junction operated at very high reverse bias voltage (1-2 kV). With the reverse bias voltage high enough, the electric field causes electrons to collide with the crystal lattice and release secondary electrons, which are in turn accelerated and produce further carrier multiplication [37].

Because we are interested in distinguishing individual particles, the response time is ideally limited only by the bandwidth of the measurement system. We would also prefer to have as much aperture as possible without compromising transient performance because, ideally, the interior of the water container would be completely surrounded by light sensors. The disadvantage of the avalanche photodiode in this respect is that as the active area increases, the junction capacitance steeply rises, thereby slowing down the response [38]. For example, the Burle 83049-542 photomultiplier we used in our design has a 76 mm aperture (4500 mm<sup>2</sup> area) and a risetime of 12 ns. To obtain similar transient performance from one of Advanced Photonix's avalanche photodiodes, we'd have to use a model with a 10 mm diameter (79 mm<sup>2</sup> active area). Forming an array of avalanche photodiodes is not feasible because the cost of one 10 mm avalanche photodiode is already far above the \$400 76 mm PMT. We chose a photomultiplier as our light detector because it maximized collecting area for total cost and maintained the desired transient performance. The device we have used throughout our work is the Burle 83049-542, which has a relatively large aperture and its high UV-blue response is well suited for sensing water Cherenkov radiation.

### 3.2 Cherenkov Radiation Measurements with the Trash Can Cherenkov Detector

At first, we were unable to observe properly the signal from the photomultiplier. The anode cable lacked a proper termination because we had believed that the signal could be measured on an oscilloscope with a standard 1 M $\Omega$  jack. We received triggers and observed the peak values of the pulses, but the peak signal was followed by an exponential decay lasting about 10 microseconds. This decay is a very large time increment for the world of high-energy physics, and it failed to represent the realistic duration of our Cherenkov radiation flashes. We obtained a digital sampling oscilloscope with the ability to electronically switch the input from the standard 1 M $\Omega$  to 50  $\Omega$ , the HP 54610 B. This eliminated the extended decay in the response by matching the characteristic impedance of the PMT anode cable. We soldered a BNC jack onto the PMT's anode cable, thereby allowing us to connect the anode to the oscilloscope with a readily available RG-58/U cable.

Our PMT assembly contains a DC step-up providing a multiplication on the order of 100 between the external supply and the dynode voltage divider network (VDN). Following the specifications of the device, we know that at an external supply voltage of 6.0 V, the VDN is powered at 860 V, resulting in an overall current gain between the cathode and the anode of  $1.5 \times 10^5$ . The maximum VDN supply for the PMT is 1500 V (10.0 V externally), resulting in a current gain of  $5 \times 10^6$ . The Pierre Auger Observatory reported in one of their experiments that a gain of  $2 \times 10^5$  is adequate for detecting water Cherenkov radiation, and suggested the use of this value in their final implementation [39]. By consulting Burle we found that this supply voltage would provide good linearity for the current amplification, a parameter that is otherwise compromised when the supply voltage is increased. We therefore chose to complete most of our experiments with an external supply voltage of 6.0 V, and we will use this value during our initial testing of the water tank installation. We have considered that characteristics specific to our detection system, such as water clarity, might necessitate a higher gain to compensate for lower photocathode excitation.

Initially, we viewed the anode pulses with the HP 54610B, but its sampling period was limited to 50 ns (despite the 500 MHz label). To observe the shape of the PMT pulses, which had widths smaller than this sampling period, we had to make use of persistence between consecutive triggers. This technique permitted us to roughly verify agreement between the observed risetimes and widths with the device's specified delta function response (12 ns and 25

ns, respectively). Fortunately, we obtained the HP 54504A, which had a true sampling period of 2.5 ns and therefore allowed a clear view of individual traces from the anode. Figures 3.1 and 3.2 below show the typical characteristics of a pulse we observed from the PMT.

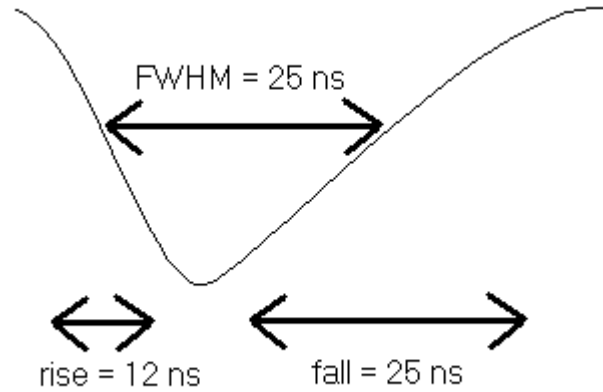


**Figure 3.1** Pulse shape diagram.

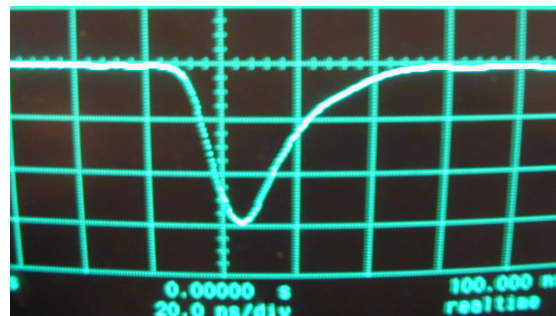


**Figure 3.2** Oscilloscope view.

The observed spectrum of full-width half-maximum (FWHM) values from a sample of 112 individual pulses observed from the PMT in the trash can Cherenkov detector is plotted in Figure 3.3. The external supply of the PMT was maintained at 6.0 V.

## FWHM versus Pulse Amplitude

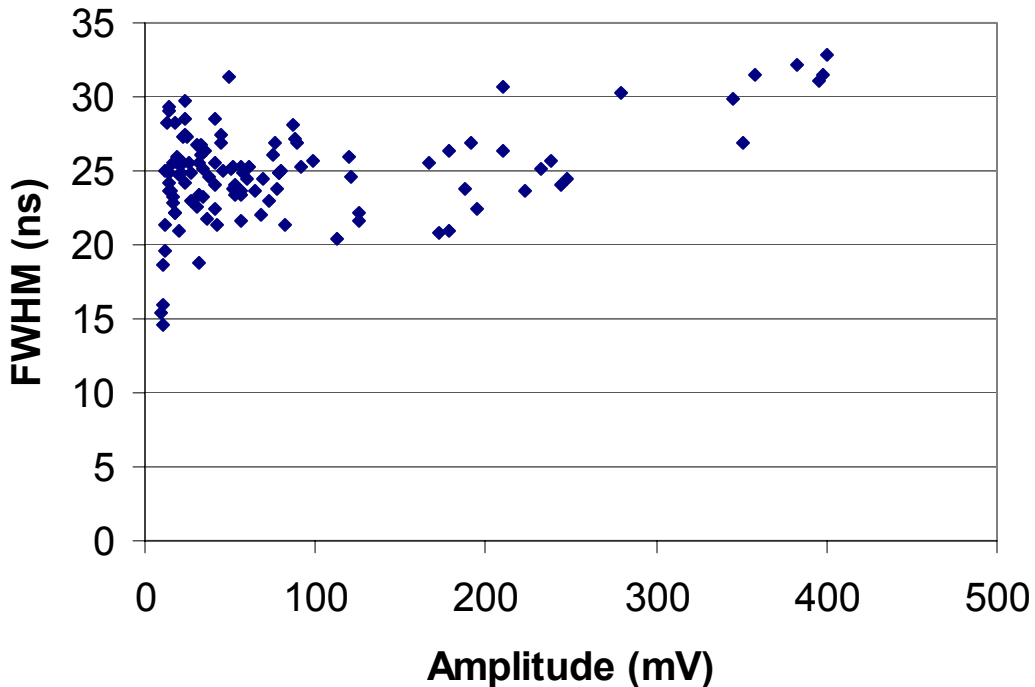


**Figure 3.3** FWHM versus amplitude.

The FWHM dependence on pulse amplitude is less significant than we had expected. That is, at amplitudes below 300 mV, the width does not scale in proportion to the height of the pulse, but instead fluctuates randomly about 25 ns. However, above 300 mV, the slope of the PMT signal reaches a ceiling, and at this point the width begins to increase. We found the maximum rising edge slope to be about 40 mV/ns. For a DAQ system that relies on time-to-digital conversion, such as the Quarknet card, knowing the intersection of the pulse with a threshold is not enough information in order to discern the shape and the amplitude of the pulse. This difficulty arises from the fact that the slope of the pulse edge varies with amplitude. Therefore, the main advantage of a high speed ADC, such as that which the Pierre Auger Observatory uses, is the greater accuracy possible in reconstructing the traces of air shower particles.

For purposes of procedure familiarization and comparison with the full-scale water tank installation, the amplitude spectrum was measured using the trash can detector. These

measurements are summarized in the logarithmic plot of Figure 2.3. The “Overall Counts” indicates the count rate of pulses with the PMT exposed to water as usual. However, the “Dark Pulse Counts” were recorded with the bulb of the trash can PMT covered in an opaque cap, and otherwise identical conditions. The significance of this information is explained in the following section. The external power supply of the PMT was maintained at 6.0 V throughout these measurements, therefore giving a current gain of  $1.5 \times 10^5$ .

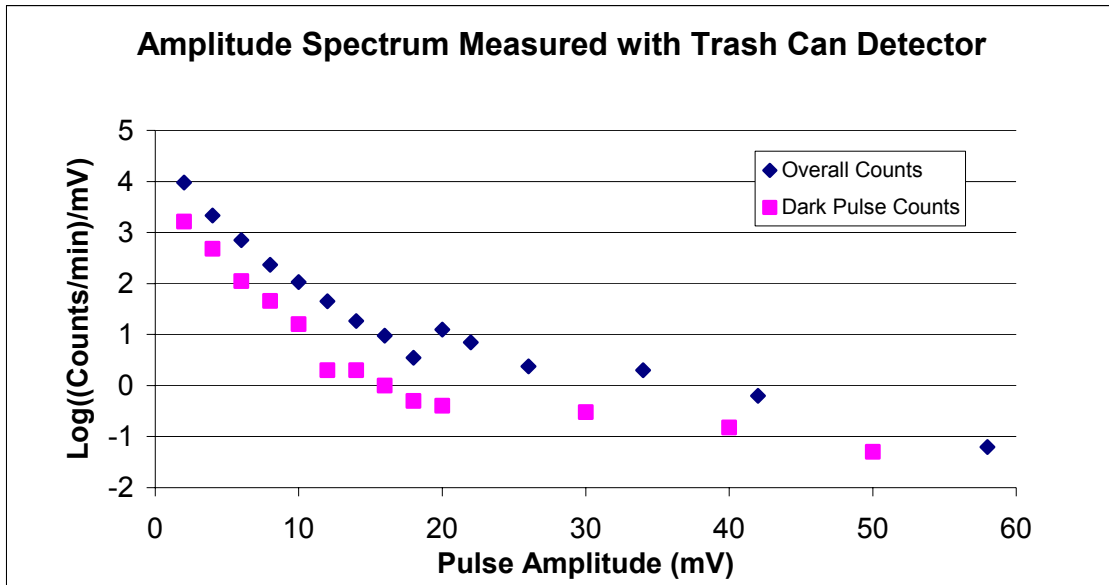


Figure 3.4 Amplitude spectrum.

### 3.3 PMT Noise

In the complete absence of light sources, every PMT creates dark pulses that increase in frequency as the gain of the device is increased. Dark pulses result from random thermionic emission of electrons at the photocathode, which are in turn amplified in the same manner as photoelectrons caused by actual light. Dark pulses are one reason why all serious cosmic ray detectors use at least 2 PMTs. With multiple PMTs sensing the Cherenkov radiation within a container, coincidence between the devices can be confirmed to ensure that dark pulses are not included in the air shower data. The amplitude spectrum plot shows that at this particular current gain,  $1.5 \times 10^5$ , the rate of dark pulses of our PMT remains around a factor of 10 below the overall pulse rate. Informal tests revealed that this dark count rate increased as the gain of the PMT was raised, as expected.

### 3.4 Single Electron Response

In order for a cosmic ray detector to be useful, we have to be able to reconstruct the arrival of particles using only the electrical signal output from its light sensors. This means we must be able to quantify the relationship between the light incident on our PMT and the current output. Therefore, the signal produced at the anode when a single photoelectron is emitted from the photocathode must be ascertained. Although the gain of our PMT is given in the data sheets in terms of [output current]/[incident luminous power], the light is quantified in power. This value would only be useful if we knew how many photons – an energy quantity – were reaching our photocathode per unit of time. Rather than calibrate our PMT with respect to a source of known power flux, we measured the single electron response for our Burle PMT, since the latter procedure included fewer experimental variables. The single electron response is the pulse that results whenever an incident photon causes a photoelectron to be ejected from the photocathode. The measurement of a single electron response proved to be a challenging experimental task. The main reason that the single electron response for our PMT was not listed in its data sheets is that the device was not designed for photon counting. It is an 8 dynode PMT, with a typical operational gain on the order of  $10^5$ . In contrast, a PMT designed for photon counting typically has a linear-region gain on the order of  $10^7$  and 12 dynodes [40].

The first method we applied to measure the single electron response is described in a photomultiplier handbook published by Philips Photonics [41]. This concept calls for the PMT to be exposed to a pulsed light source, attenuated enough so that when the source is on, the cathode sparsely emits photoelectrons. With such a small amount of light incident on the photocathode, the majority of the pulses can be attributed to single electrons. The oscilloscope is externally triggered by the signal pulsing the light source, to greatly reduce the probability of looking at dark pulses. For our pulsed light source we used an LED, wrapped in successive layers of electric tape. The PMT was contained in an aluminum box. Attenuating the LED and observing the corresponding changes in the anode signal, we found that we were unable to reduce the continuous response of the PMT into a series of pulses before the response became buried in the 2 mV noise of our oscilloscope.

After further investigation, we found that in one study conducted by the Pierre Auger Observatory, researchers used cosmic ray EAS particles to find the single electron response [42]. In this setup, one detector PMT triggers an oscilloscope, so that the signal caused by a crossing

particle can also be viewed on a separate PMT in an adjacent detector. However, the second PMT is masked so that less than one hundredth of its total photocathode area is exposed to radiation. This reduces the probability of photoelectron emission to the point where for most crossing particles a signal will not even register. Therefore, any emission from the second PMT upon the triggering of a crossing particle is predominantly caused by emission of just one photoelectron. Our adaptation of this technique is shown in Figure 3.4.

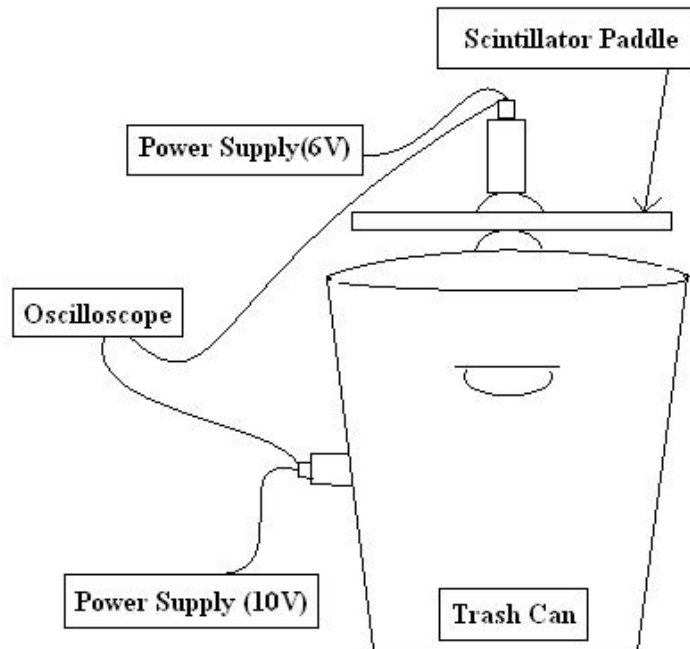


**Figure 3.4** Setup for measuring single electron response.

The PMT in the trash can was externally powered at the maximum rated supply voltage, 10.0 V, yielding a gain of  $5.3 \times 10^6$ . The scintillator detector was externally powered at 5.0 V. Using the scintillator pulses to trigger the oscilloscope, the output of the trash can PMT was observed to occasionally yield small pulses with amplitudes at a mean of about 10 mV. An image of several single electron pulses is shown in Figure 2.5. The lower half of the display corresponds to Channel 1, the single electron pulses viewed from the trash can PMT. The upper half (at a much larger Volts/division setting) is Channel 2, the scintillator triggers. Scaling down the gain to the normal operating value of  $1.5 \times 10^5$ , we expect the amplitude of a single photoelectron to be about 0.3 mV. Such a small amplitude pulse would not have been visible in the noise of the oscilloscope if this experiment were done with an external supply of 6.0 V.

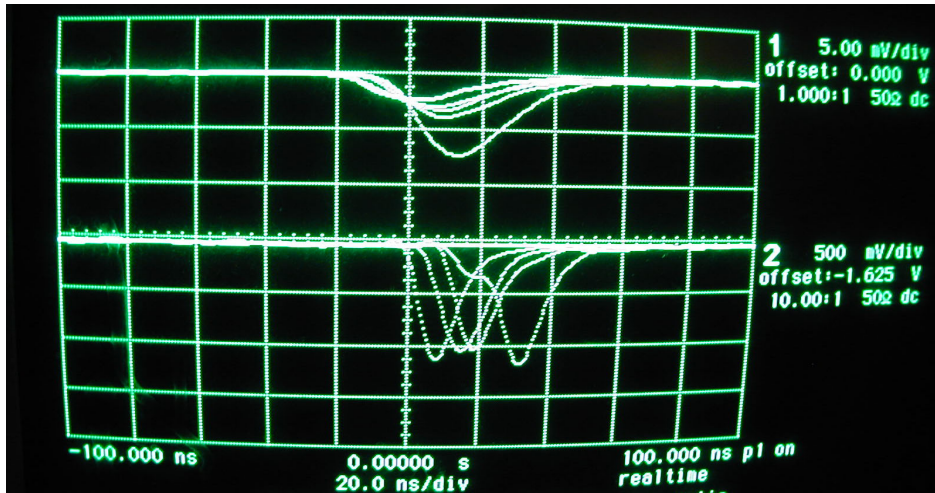


**Figure 3.5** Oscilloscope view of single electron response.

### 3.5 Water Transmittance

Unlike the Pierre Auger Observatory, the use of purified water is not an option for this experiment, since we are using tanks that are pumped with domestic drinking water for our experiments. Therefore we set out to compare the transmission spectrum of NYC tap water with the theoretical Cherenkov radiation spectrum. Using a UV/Visible spectrophotometer with a 1 cm path length cuvette, we measured the transmittance of a sample of the Cooper Union Engineering Building's tap water with respect to high purity water between 300 and 500 nm. The results are plotted in Figure 3.6.

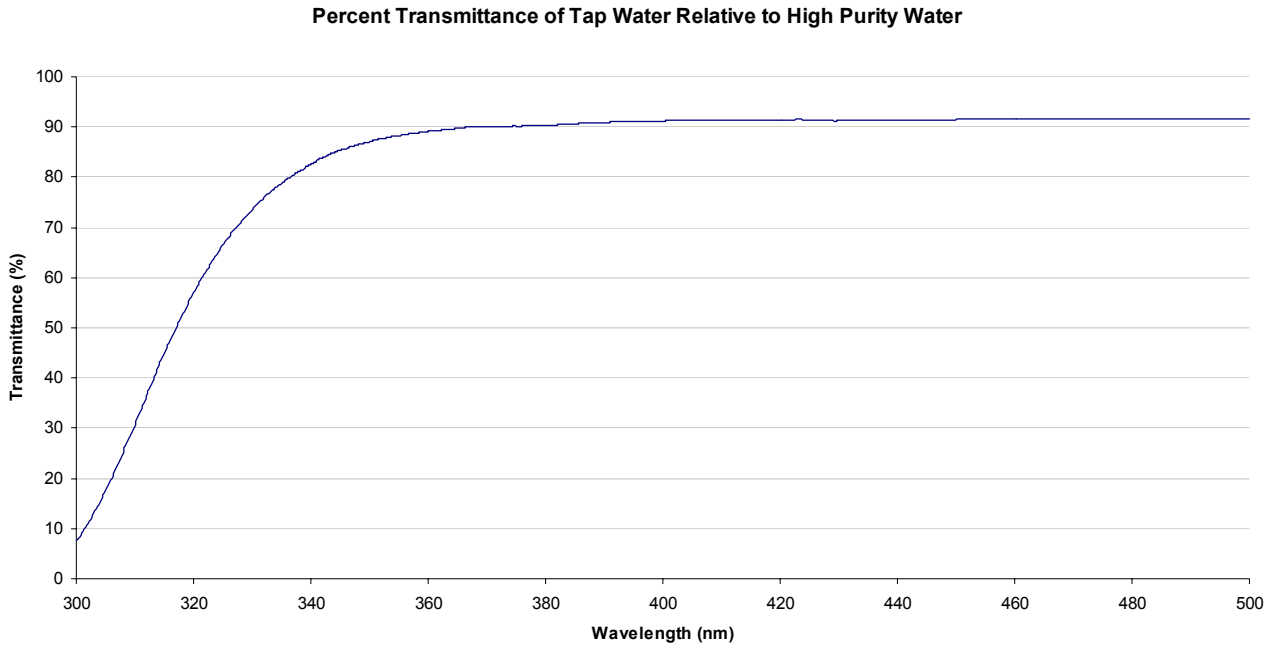


**Figure 3.6** Tap water transmittance.

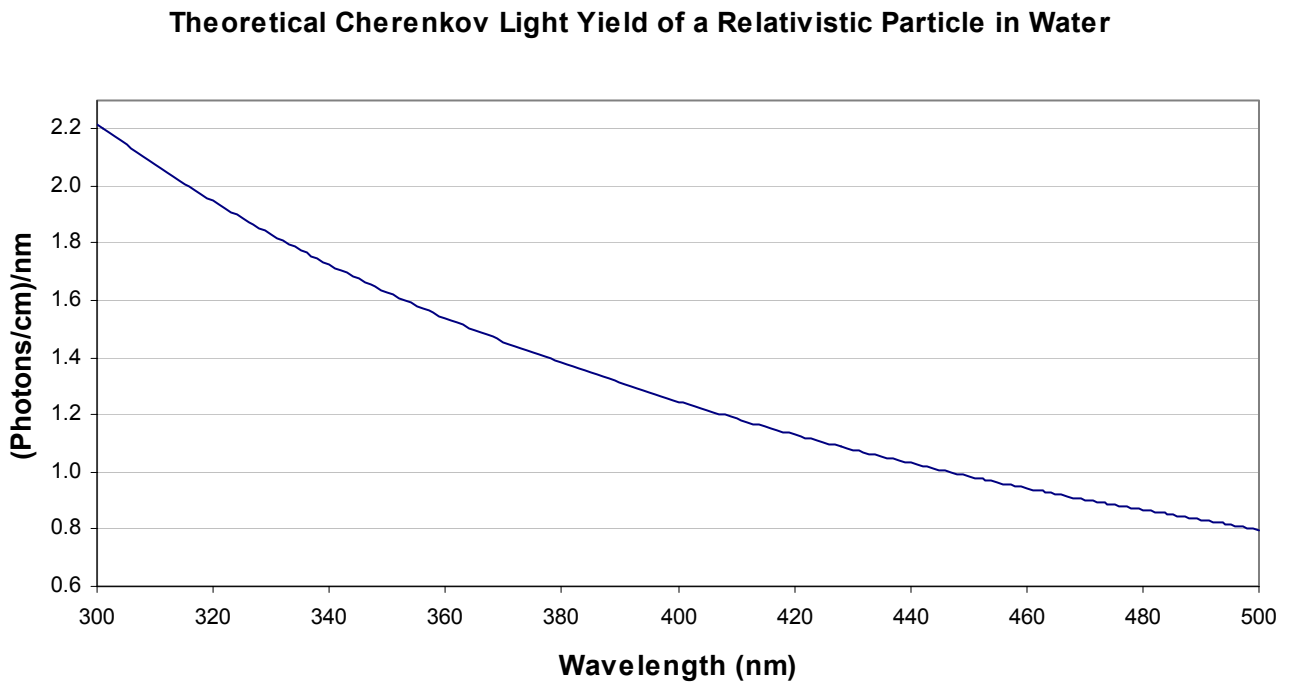


**Figure 3.7** Theoretical Cherenkov light yield.

The measured transmittance agrees with established research on the optical properties of tap water. The presence of metal ions, microbes, and other dissolved solids steeply reduce the transmittance of the tap water sample in the UV region. Figure 3.7 demonstrates the theoretical yield of Cherenkov radiation, using equation 1.1 and approximating the speed of the particle as  $c$  (a typical muon has an energy of about 1 GeV), in terms of how many photons are released per centimeter of path length per nanometer wavelength interval. The transmittance of tap water is of great concern because it could possibly counteract the benefit of having a large tank volume. For example, a 0.9 transmittance over a path length of 1 cm becomes  $0.9^{100} = 0.00003$  over a path length of 1 m. Further investigation of the optical effects of dissolved solids in domestic water on the propagation of Cherenkov radiation should be completed in the near future.

## *Chapter 4: Photomultiplier Pre-Amplifier*

All photomultipliers acting in pulsed radiation mode can be modeled as current sources [43]. The output signal from the PMT travels a significant distance (about 30 feet for the tank on the Engineering building) before reaching the data acquisition system on the rooftop. We decided to use a pre-amplifier at the base of the PMT, in order to isolate the load presented by the coaxial cable. In particular, the pre-amplifier buffers the PMT from the coaxial cable's parasitic capacitance, which would otherwise impair the transient characteristics of the Cherenkov radiation pulses. The RG-58/U type cable typically has a capacitance of 30 pF/ft, and so a length of cable of about 50 feet would result in 1.5 nF.

Although pre-amplifiers designed for photomultiplier applications were available from manufacturers such as Ortec, we sought alternatives which were lower in price. General electronics manufacturers offered a variety of low priced, high speed ICs readily available, along with their corresponding evaluation boards. The main consideration in the selection process was to identify devices with suitable bandwidth for the Cherenkov signals present at the anode of our PMT. The bandwidth of a signal can be estimated as  $0.35/\text{risetime}$ , and after observing an average risetime of 10 nanoseconds in the Cherenkov pulses from our Burle PMT, we estimated the 3 dB bandwidth of our signal to be 35 MHz. This value is comparable to the Pierre Auger Observatory sampling rate of 40 MHz – Nyquist sampling criterion implies that they designed their detector with a similar signal bandwidth in mind.

We selected and tested three different amplifiers. The Analog Devices 8011 and 8001 are current feedback op-amps. The third, the National Semiconductor LMH 6559, is a unity gain buffer with an internal closed loop. We designed the current feedback op-amp circuits as 10x non-inverting amplifiers. For all three ICs we used  $49.9\ \Omega$  resistors at the input and output terminals to match the impedances of the adjoining coaxial cables. Using rosin paste and flux with a hot air gun, we soldered each of the ICs (all in SOIC packages), along with their corresponding passive surface mount components, onto the evaluation circuit boards (see Figure 4.1). Since all three of the evaluation boards already had  $50\ \Omega$  microstrip traces for the terminals of each device, the last step was to solder edge-mount SMA connectors onto the appropriate pads. To verify the input impedance, output impedance, conductivity of the surface mount connections, and to ensure that there were no accidental shorts between IC pins, we probed all

three of the evaluation boards with a multimeter. The application of a low frequency signal generator to the input allowed us to verify the basic functionality of each amplifier. However, before testing the amplifiers at higher frequencies, we decided that it would be best to construct the 30 ft coaxial cables that would be used for the tank setup of the Engineering building tank. Using the coaxial cables, we could then determine the cumulative response of the entire signal path.

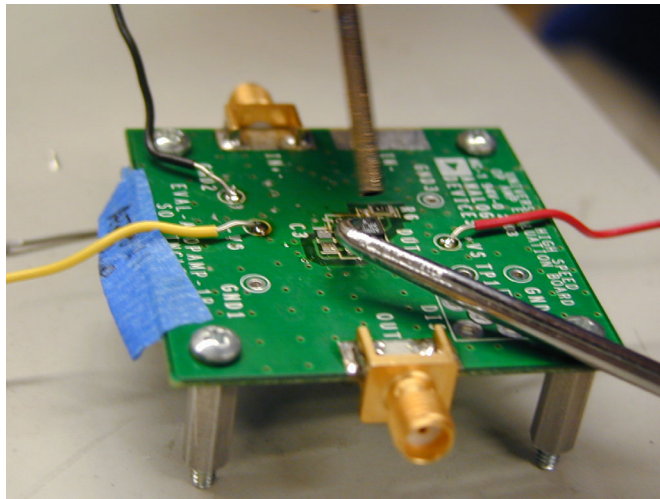


**Figure 4.1** PC board mounting.

We chose the RG 58/U type of cable to carry the signal from the pre-amplifier to the DAQ system for its affordability, frequency response, mechanical flexibility, and ease of adaptability to BNC interconnects. At 50 MHz, the typical attenuation per 100 feet of RG 58/U cable is listed as about 3 dB. We found this level of loss to be acceptable considering a 3 dB signal bandwidth of 35 MHz, and the fact that it would make extra cable length admissible in case a different setup requires more than 50 feet. Although we would have preferred to crimp the BNC plugs onto the cables, the laboratory did not have a crimping tool available. Instead, we resorted to using solder-on BNC plugs.

To test the frequency response of the amplifiers, we connected the RF output of a signal generator (Agilent E4432B) to the SMA input jack of a given amplifier. We connected one of our 30 ft coaxial cables between the output of the amplifier and the RF input of a spectrum analyzer (HP 8590A). After setting the output of the signal generator to a level of  $-50$  dBm, we swept the signal 250 kHz to 500 MHz, and recorded the 3 dB point of the frequency response.

The 30 ft RG 58/U coaxial cable by itself had a 3 dB point of 400 MHz, which was in agreement with the manufacturer's specification of 10.1 dB loss per 100 feet at this frequency. As was expected, the response for the LMH 6559 unity gain buffer, which was specified with a 1750 MHz closed loop bandwidth, was limited only by the 30 ft coaxial cable. The setup with the AD 8001 indicated a 3 dB point at 290 MHz, which matched the bandwidth listed in the data sheets for a non-inverting gain of 10. In fact, the only amplifier that did not perform to specification was the AD 8011, which displayed a 3 dB point at 64 MHz, instead of the expected value of 100 MHz. The reason for the flaw in operation of the AD8011 was not investigated because it was apparent that the AD 8001 would operate satisfactorily as a pre-amplifier.

Originally, the only major drawback of the LMH 6559 appeared to be its lack of voltage gain capability. This flaw became apparent when, in order to match the impedance of the device output to the coaxial cable, a 50  $\Omega$  resistor was placed in series with the output node. This resistor created a voltage divider across the output of each device, so that in the case of the unity gain buffer the signal reaching the load was actually half that of the PMT anode. Similarly, the gain for the 10x non-inverting circuits was effectively only 5. However, concurrent experiments with the trash can Cherenkov detector revealed that pulse amplitude from the PMT was not a problem, since at standard PMT supply voltages the background EAS particles appeared to generate signals at the minimum on the order of 10 mV. The value 10 mV is above the noise amplitude of any reasonable data acquisition system, including the Quarknet card we are using. Therefore, the attenuation caused by the LMH 6559 is not a problem. One practical advantage of the LMH 6559 over the other amplifiers tested is the simplicity of its assembly onto a PC board, since the feedback loop is built into the IC. In addition to previous considerations, the LMH 6559's exceptional bandwidth led us to conclude that the LMH 6559 is the best choice for the PMT pre-amplifier.

## *Chapter 5: Water Tank Detector Housing*

We determined that the simplest way to sense Cherenkov radiation in a utility water tank is to have the PMTs fixed in place on the floor of the tank, facing upwards. Early on we rejected the idea of cutting holes in the floor or walls of the tank. Viewing the water from above, although requiring less signal path length, requires moving the detector along with the changing water level, if the depth of water in view is not being compromised. Therefore, in our detection design, the housing of the photomultiplier serves to hold the device in place on the floor of the tank, and seal it from water.

In the context of an array, the design for the photomultiplier housing had to be simple; easy construction enables consistent replication in each tank. Durability was also an issue since deployments would hypothetically be submerged for years without maintenance. The most challenging constraint, however, was that all of the materials in contact with water had to be officially approved for submersion in potable water systems.

The form of the housing went through several stages of evolution. Initially a die-cast stainless steel box was chosen for its ability to enclose the photomultiplier in a watertight container, while providing mechanical support. Stainless steel was known to be safe for potable water and the remaining task was to find a safe form of epoxy, caulk, or waterproof glue that would be appropriate for the connections of cables to the box. In this design, the cables would be enclosed in rubber jackets. However, after many phone calls to companies and research on industry websites, we found that there is no sealant or adhesive to bond the steel to the rubber jackets that meets health requirements of potable water. Specifically, we wanted our materials to meet National Sanitation Foundation (NSF), which is the most widely recognized authority in the field of material safety testing. The NSF standard 61 applies to drinking water system components.

Because of the lack of approved sealants, we decided that a better means of sealing the electronics from the water would be to use a single piece of plastic film enclosing each PMT along with its cables. We would still use a die-cast box to support the PMT, but in this design plastic fully surrounded the box, acting as a water barrier. For bulkhead BNC connections to the die-cast box, we drilled three holes – one for the buffered signal from the PMT, and two for the power supply. We hollowed out a beveled, 2 inch circular hole to snugly fit the collar of the

83049-542 photomultiplier bulb (see Figure 5.1). Samples of clear, FDA approved polyethylene were evaluated and a heat sealable polyethylene plastic sleeve was chosen as the barrier (see Figure 5.2).

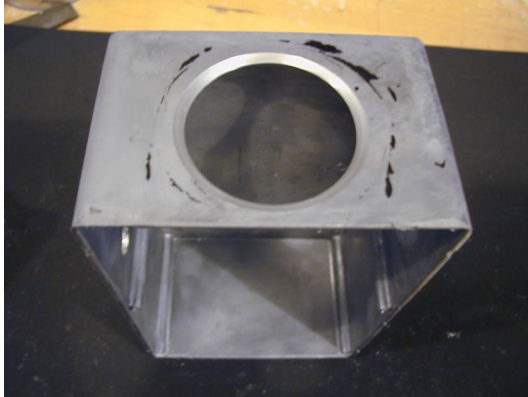


**Figure 5.1** Die-cast box for PMT.



**Figure 5.2** Polyethylene sleeve.

After further evaluation of the plastic, there arose concerns about durability and safety. Although polyethylene was FDA approved, it lacked National Sanitation Foundation approval. Such films are not intended to be left in contact with the food for years at a time. Therefore it was conceivable that we would find long term chemical resistance problems.

Revisiting research on PVC pipe as an alternate enclosure, we discovered that transparent PVC pipe and fittings were commercially available. We quickly accepted this as the best method for deployment, since it provided a waterproof enclosure that would allow light to enter as well as meeting all conceivable potable water safety requirements. We housed two PMTs in a pipe structure constructed of readily available schedule 40 PVC pipe components. In this design, the PMTS were positioned so that they face upwards from the floor of the tank (see Figure 5.3 - 5.5). We used readily available NSF 61 labeled primer and solvent cement to permanently adhere the assorted pipes and fittings. The wide canisters that contain the PMT are 3 inch inner diameter pipe sections – slightly wider than the Burle PMT. Foam sheets lining the inside of the canister exert pressure on the PMT to firmly secure it in place. We filled the space between the photocathode of the PMT and the PVC cap with silicone optical grease. By replacing the air in this gap with a medium of a higher refractive index, approximately equal to 1.5, the refraction angle at the boundary between the PVC and the gap is reduced.

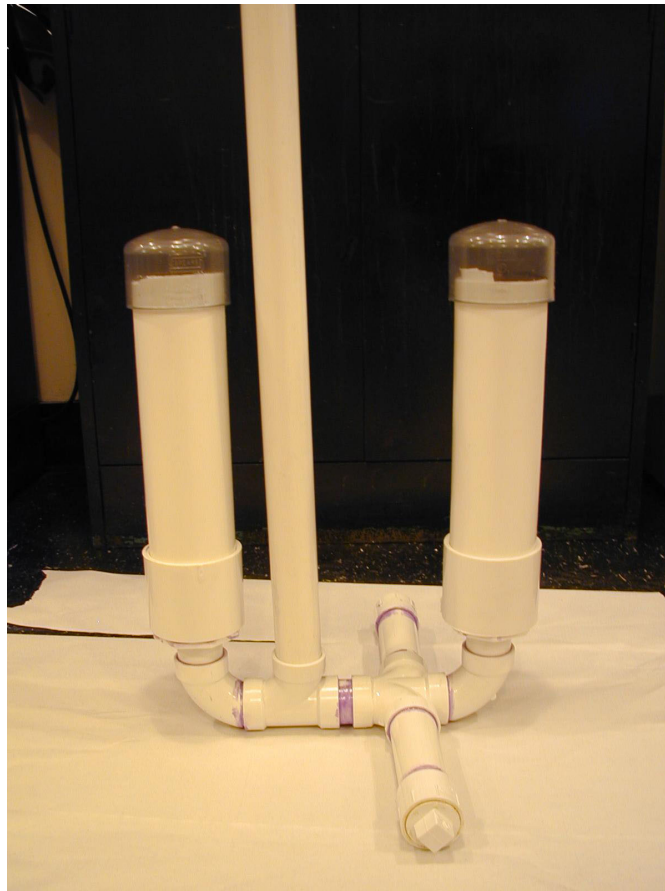


**Figure 5.3** PVC PMT housing.



**Figure 5.4** PVC PMT Housing.

One problem with this first PVC design is that the cap over each PMT exhibits significant light transmission loss. We cut a small sample of a PVC cap and measured its absorption spectrum with a UV/visible spectrophotometer. The result is plotted in Figure 5.4. It shows that the transmittance is 70% at best, for blue light, but drops steeply into the violet range. After further research we found that this high violet absorption is common to most plastics. However, one exception to this is acrylic plastic, which has excellent transmittance throughout the visible and UV range [44]. On the NSF database we were able to find one solvent cement that bonds PVC to acrylic and meets NSF 61 – Loctite Hysol H4000. After testing the efficacy of such cement in creating a watertight seal between a thin disk of extruded acrylic and the end of a PVC pipe, we will hopefully be able to replace the PVC caps and thereby improve the overall performance of the detector.

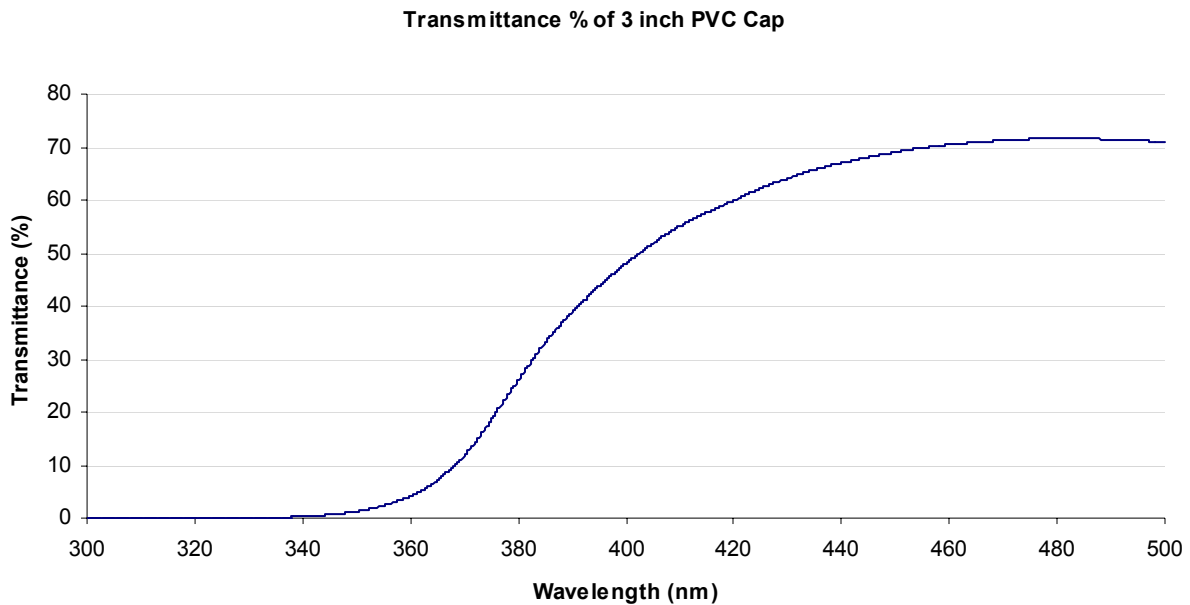


**Figure 5.4** PVC cap transmittance.

After the housing is installed in a water tank (Figure 5.5), the first measurement that should be made is the vertical muon response. The vertical muon response is a yardstick of sensitivity for a water Cherenkov detector. Together with the single electron response of the PMT, this value would be used in computer simulations to predict behavior of the detector upon the arrival of an air shower. Our measurement of vertical muon response will be accomplished using two scintillators positioned in a column so that they will only show coincidence for

particles crossing with nearly vertical trajectories, as shown in Figure 5.6. In addition, amplitude spectrum measurements such as those conducted for the trash can detector would be repeated.

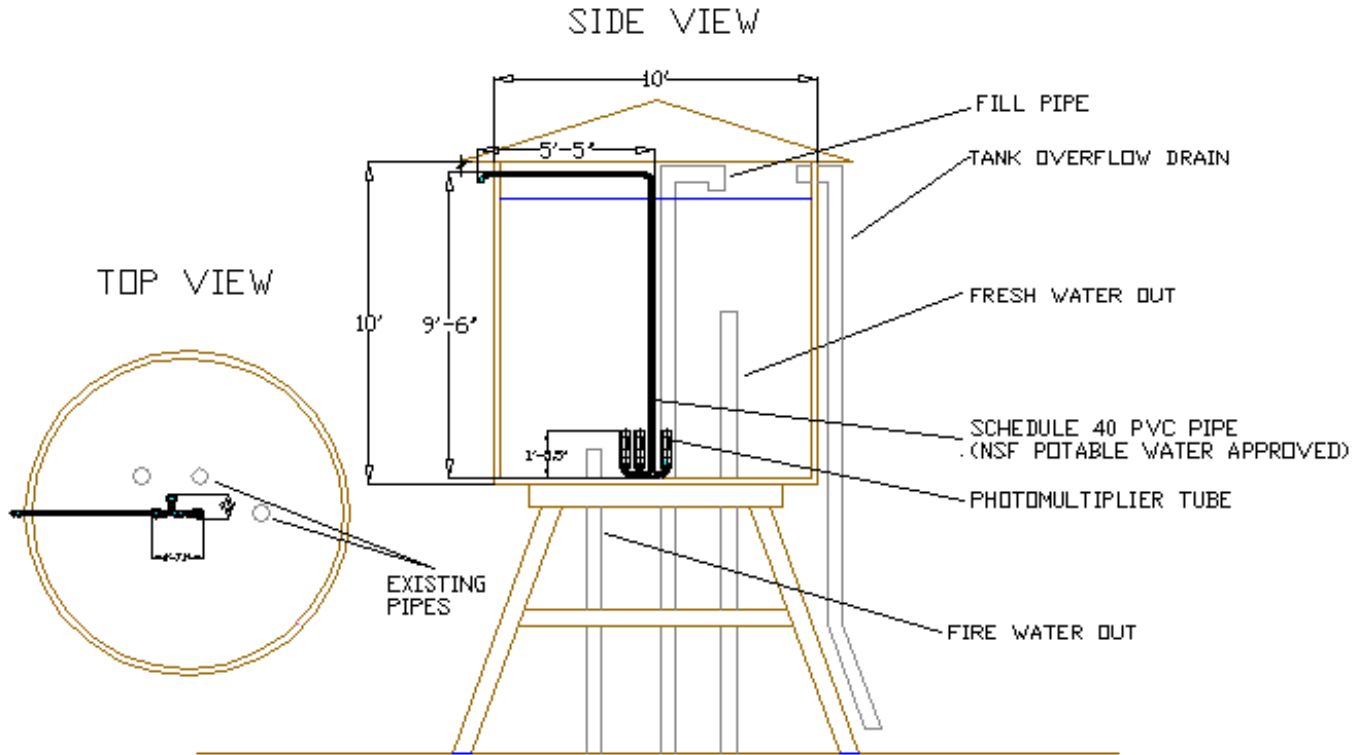


**Figure 5.5** PMT housing installation for a typical NYC wooden tank.

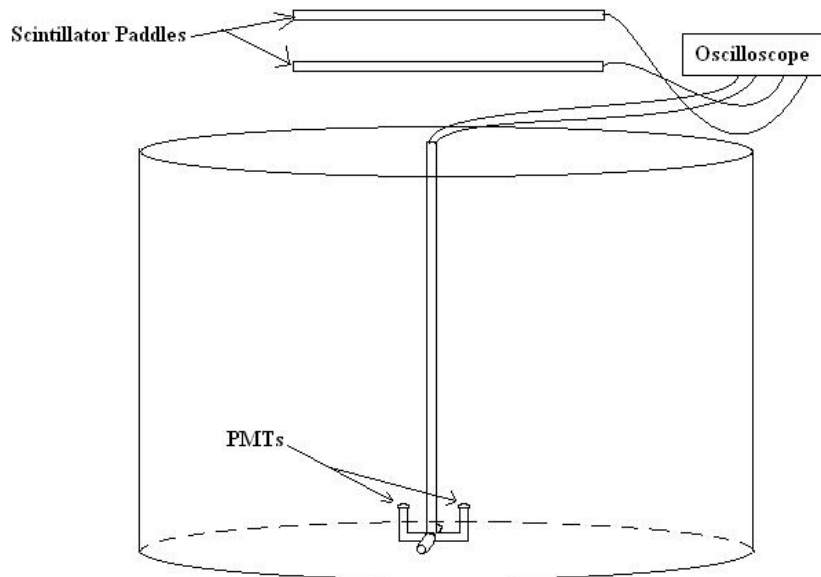


**Figure 5.6** Setup for vertical muon response.

## *Conclusion*

NYC rooftop water tanks present a compelling infrastructure for an array of detectors to study ultra high energy cosmic ray events. Using a trash can particle detector as a workbench we have characterized the response of a photomultiplier tube to Cherenkov radiation. We have designed and tested a voltage pre-amplifier circuit to isolate the photomultiplier from the capacitance of a long coaxial cable. We have designed and constructed an enclosure for the PMTs that satisfies our functional and safety requirements. We will soon install our detector in a wooden water tank, and demonstrate the value of further pursuit in this endeavor.

## *Acknowledgements*

There are quite a few people who went out of their way to assist us in this project. We thank our advisor, Toby Cumberbatch, for his technical guidance and encouragement. We especially acknowledge Glennys Farrar of NYU for providing the inspiration for this undertaking. We also thank Glenn Gross, Jeff Hakner, and Roy Belton, who repeatedly shared their electrical engineering expertise and helped us overcome numerous practical problems. We owe much to Mike Eilenfeldt for his help in various construction aspects. Michelle Noris, a Cooper Union Civil Engineering alumna was invaluable in giving us advice for making our design safe and helping us in our attempt to obtain city approval. For their generosity in sharing valuable equipment and photomultiplier expertise, we thank Stefan Westerhoff and Brian Connolly of Columbia University, and John Martin of Burle Industries.

- 
- [1] Stephen A. Bull. (2001). *Where Do Cosmic Ray Come From?* Retrieved October 15, 2003, from University of Birmingham:  
<http://www.ep.ph.bham.ac.uk/general/SparkChamber/text5h.html>
- [2] G. Henri. (1999). *Active Galactic Nuclei As High Energy Engines*. Retrieved Dec 5, 2003 from arXiv.org e-Print archive:  
[http://arxiv.org/PS\\_cache/astro-ph/pdf/9901/9901051.pdf](http://arxiv.org/PS_cache/astro-ph/pdf/9901/9901051.pdf)
- [3] Enrico Fermi. (2003). *History of Cosmic Ray Research*. Retrieved October 15, 2003, from Slovene Pierre Auger Observatory Site:  
<http://www.p-ng.si/public/pao/history.php>
- [4] Chris Waltham. (2003). *Where Do Cosmic Rays Come From?* Retrieved October 15, 2003, from University of British Columbia:  
[http://www.physics.ubc.ca/~outreach/phys420/p420\\_99/flora/wheredo.html](http://www.physics.ubc.ca/~outreach/phys420/p420_99/flora/wheredo.html)
- [5] Josh Plaut. (1998). *NYU Physicist Proposes New Theory For Origin And Make-Up Of Extremely High-Energy Cosmic Rays*. Retrieved Dec 5, 2003 from NYU Press:  
[http://www.nyu.edu/publicaffairs/newsreleases/b\\_NYU\\_P8.shtml](http://www.nyu.edu/publicaffairs/newsreleases/b_NYU_P8.shtml)
- [6] Matthew Silver. (May, 1999) *Gamma Ray Astronomy*. Retrieved Dec 5, 2003 from Williams College:  
<http://www.williams.edu/Astronomy/Course-Pages/418/MRSpaper.html>
- [7] G. Farrar. (2002). *Ultra High Energy Cosmic Rays*. Retrieved December 15, 2003, from New York Schools Cosmic Particle Telescope:  
<http://www.physics.nyu.edu/NYSCPT>
- [8] *Where do Cosmic Rays come from?*. (n.d.). Retrieved October 14, 2003, from University of Leeds: <http://ast.leeds.ac.uk/haverah/origin.shtml>
- [9] *Meson*. (n.d.). Retrieved December 16, 2003, from Wikipedia:  
<http://en2.wikipedia.org/wiki/Meson>
- [10] Konrad Bernlöhr (n.d.). *Cosmic-ray air showers*. Retrieved March 28, 2004, from Max Planck Institute: <http://www.mpi-hd.mpg.de/hfm/CosmicRay/Showers.html>
- [11] The Auger Collaboration. (1997 March) *The Pierre Auger Observatory Design Report*, Pierre Auger Observatory. [Online]. Available:  
<http://www.auger.org/admin/DesignReport/index.html>, p. 70.
- [12] M. A. Pomerantz, p. 36.

- 
- [13] C. N. Booth. (n.d.). *Coherent Effect for Charged Particles*. Retrieved October 14, 2003, from University of Sheffield:  
<http://www.shef.ac.uk/physics/teaching/phy311/coherent.html>
- [14] The Auger Collaboration, p. 115.
- [15] P. Sokolsky, *Introduction to Ultrahigh Energy Cosmic Ray Physics*. Redwood City, CA: Addison-Wesley Publishing Company, 1989, p. 15.
- [16] Ibid, p. 16.
- [17] J. Wdowczyk, "Extensive air showers below 10 eV," in *Cosmic Rays at Ground Level*, A. W. Wolfendale, Ed. London: The Institute of Physics, 1973, p. 146.
- [18] P. Sokolsky, p. 39.
- [19] *A New Astrophysics Facility Rises from the Pampa*. (n.d). Retrieved October 14, 2003, from Pierre Auger Observatory: <http://www.auger.org/overview.html>
- [20] B. McShane. (2002, May). *In New York, the water is aged in barrels*. Retrieved October 14, 2003, from Columbia News Service:  
<http://www.jrn.columbia.edu/studentwork/cns/2002-05-15/645.asp>
- [21] Ibid.
- [22] A. Kreda. (1997 June). *Sprucing up a piece of Americana*. Retrieved October 14, 2003, from Southcoast Today: <http://www.s-t.com/daily/06-97/06-29-97/f01bu195.htm>
- [23] B. McShane.
- [24] *Water tower*. (n.d.). Retrieved October 14, 2003 from Urban75:  
<http://www.urban75.org/photos/newyork/ny155.html>
- [25] (2003 May). *Ask the Engineer: Fixing Brown Water and Low Pressure*. Retrieved October 14, 2003, from Rand Engineering:  
<http://www.randpc.com/AskTheEngineer/rooftank.htm>
- [26] B. McShane.
- [27] G. Farrar. (2002). *Ultra High Energy Cosmic Rays*. Retrieved October 14, 2003, from New York Schools Cosmic Particle Telescope:  
[http://physics.nyu.edu/~farrar/research/NYU\\_030202\\_files/frame.htm](http://physics.nyu.edu/~farrar/research/NYU_030202_files/frame.htm)

- 
- [28] *A New Astrophysics Facility Rises from the Pampa.* (n.d.). Retrieved October 14, 2003 from Pierre Auger Observatory: <http://www.auger.org/overview.html>
- [29] The Auger Collaboration, p. 110.
- [30] *A New Astrophysics Facility Rises from the Pampa.*
- [31] The Auger Collaboration, p 152.
- [32] M. A. DuVernois, "GAP-98-007 Notes on Global Navigation Satellite Service (GNSS)," Auger Observatory, GAP-98-007, 1998.
- [33] P. Enge, "Retooling the Global Positioning System," *Scientific American*, pp. 91-97, May 2004.
- [34] Ibid.
- [35] *Information about Super-Kamiokande.* (n.d). Retrieved April 13, 2004, from University of California, Irvine: <http://www.ps.uci.edu/~superk/sk-info.html>
- [36] D. Washington. (2002). *Mounting a Scintillation Detector.* Retrieved March 30, 2004, from Columbia University: <http://www.nevis.columbia.edu/reu/2002/manual.pdf>
- [37] B. Koren. (n.d.). *A Primer on Photodiodes.* Retrieved May 3, 2004, from Advanced Photonix: [http://www.advancedphotonix.com/word\\_docs/PRIMER\\_OE\\_Magazine\\_.doc](http://www.advancedphotonix.com/word_docs/PRIMER_OE_Magazine_.doc)
- [38] Centrovision. (n.d.) *A Primer on Photodiode Technology.* Retrieved May 3, 2004, from Centrovision: <http://www.centrovision.com/tech2.htm#circuits>
- [39] T. Suomijarvi, "Processing of Signals from Surface Detectors of the Auger Observatory," in *28th International Cosmic Ray Conference.* Universal Academy Press, Inc., 2003, pp 473-476. Available: [http://www.auger.org/icrc2003/signal\\_processing.pdf](http://www.auger.org/icrc2003/signal_processing.pdf)
- [40] Ortec. (n.d.) *Application Note 51: Pulse-Processing Electronics for Single Photon Counting.* Retrieved March 27, 2004 from Ortec: <http://www.ortec-online.com/pdf/an51.pdf>
- [41] Philips Photonics. *Photomultiplier Tubes: Principles and Applications.* Brive, France: Philips Photonics, 1994, pp 4.12 – 4.13.
- [42] D. Ravignani, "GAP-97-024 Calculation of the Number of Photoelectrons with the Water Cherenkov Detector Model," Pierre Auger Collaboration. Apr. 1997. Available: [http://www.auger.org/admin-cgi-bin/woda/gap\\_notes.pl](http://www.auger.org/admin-cgi-bin/woda/gap_notes.pl)

- 
- [43] Philips Photonics. *Photomultiplier Tubes: Principles and Applications*. Brive, France: Philips Photonics, 1994, pp 5.21 – 5.22.
- [44] W.A. Whitaker. (1996). *Acrylic Polymers: a Clear Focus*. Retrieved May 6, 2004 from Medical Device Link: <http://www.devicelink.com/mpb/archive/96/01/001.html>